NANO MICRO
small

Postfach 10 11 61
69451 Weinheim
Germany
Courier services:
Boschstraße 12
69469 Weinheim
Germany
Tel.: (+49) 6201 606 235 / 432
Fax: (+49) 6201 606 500
E-mail: small@wiley-vch.de

WILEY-VCH

Dear Author,

Please correct your galley proofs carefully and return them no more than three days after the page proofs have been received.

If you have not used the PXE system before, please view the Tutorial before checking your proofs: http://wileypxe.aptaracorp.com/pxewileyvch/UserDocument/UserGuide/WileyPXE5_AuthorInstructions.pdf

Please note any queries that require your attention. These are indicated with red Qs in the pdf or highlighted as yellow queries in the "Edit" window.

Please pay particular close attention to the following, as no further corrections can be made once the article is published online:

- **Names** of all authors present and spelled correctly
- **Titles** of authors are correct (Prof. or Dr. only: please note, Prof. Dr. is not used in the journals)
- **Addresses of all authors** and **e-mail address of the corresponding author** are correct and up-to-date
- **Funding bodies** have been included and grant numbers are accurate
- The **Title** of the article is OK
- All **figures** are correctly included
- **Equations** are typeset correctly

Note that figure resolution in the PXE system is deliberately lower to reduce loading times. This will be optimized before the article is published online.

Please send any additional information, such as figures or other display items, to small@wiley-vch.de, and please also indicate this clearly in the PXE "Edit" window by inserting a comment using the query tool.

Reprints may be ordered by filling out the accompanying form.
Return the reprint order form by e-mail with the corrected proofs, to Wiley- VCH: **small@wiley-vch.de**

Please limit corrections to errors already in the text. Costs incurred for any further changes will be charged to the author, unless such changes have been agreed upon by the editor.

The editors reserve the right to publish your article without your corrections if the proofs do not arrive in time. Note that the author is liable for damages arising from incorrect statements, including misprints.

NANO MICRO small

Editorial Office:

Wiley-VCH Verlag, Boschstrasse 12
69469 Weinheim, Germany

Tel.: (+49) 6201 606 235
Fax: (+49) 6201 606 500

E-mail: small@wiley-vch.de
http://www.small-journal.com

Reprint Order Form 2015
- please return with your proofs -

Manuscript No. _____

Please send me and bill me for

☐ no. of **reprints** via ☐ airmail (+ 25 Euro) ☐ surface mail

☐ no. of **copies of this issue** (1 copy: 25 Euro) via ☐ airmail (+ 25 Euro) ☐ surface mail

☐ **high-resolution PDF file** (330 Euro).
My e-mail address:

_____

Please note: It is not permitted to present the PDF file on the internet or on company homepages

★**Special Offer**★ If you order 200 or more reprints you will get a PDF file for half price.

Information regarding VAT
Please note that from German sales tax point of view, the charge for **Reprints, Issues or Posters** is considered as **"supply of goods"** and therefore, in general, such delivery is a subject to German sales tax. However, this regulation has no impact on customers located outside of the European Union. Deliveries to customers outside the Community are automatically tax-exempt. Deliveries within the Community to institutional customers outside of Germany are exempted from the German tax (VAT) only if the customer provides the supplier with his/her VAT number. The VAT number (value added tax identification number) is a tax registration number used in the countries of the European Union to identify corporate entities doing business there. It starts with a country code (e.g. FR for France, GB for Great Britain) and follows by numbers.

Mail reprints /cover posters / copies of the issue to:

_____
_____
_____
_____
_____

Invoice address:

_____
_____
_____
_____
_____

_____
Date, Signature **Stamp**

VAT no.: _____
(institutes / companies in EU countries only)

Purchase Order No.: _____

Credit Card Payment

VISA, MasterCard, AMERICAN EXPRESS
Please use the Credit Card Token Generator located at the website below to create a token for secure payment. The token will be used instead of your credit card number.

Credit Card Token Generator:
https://www.wiley-vch.de/editorial_production/index.php

Please transfer your token number to the space below.

Credit Card Token Number:

Cover Posters

Posters are available of all the published covers and frontispieces in two sizes

☐ DIN A2 42 x 60 cm / 17 x 24in (one copy: **39 Euro**)
☐ DIN A1 60 x 84 cm / 24 x 33in (one copy: **49 Euro**)

Postage for shipping posters overseas by airmail:
+ 25 Euro

Postage for shipping posters within Europe by surface mail:
+ 15 Euro

Price list for reprints (The prices include mailing and handling charges. All Wiley-VCH prices are exclusive of VAT)

No. of pages	Price (in Euro) for orders of 50 copies	100 copies	150 copies	200 copies	300 copies	500 copies
1-4	345	395	425	445	548	752
5-8	490	573	608	636	784	1077
9-12	640	739	786	824	1016	1396
13-16	780	900	958	1004	1237	1701
17-20	930	1070	1138	1196	1489	2022
for every additional 4 pages	147	169	175	188	231	315

★ **Special Offer** ★ If you order 200 or more reprints you will get a PDF file for half price.

Wiley-VCH Verlag GmbH & Co. KGaA; Location of the Company: Weinheim;
Chairman of the Supervisory Board: Stephen Michael Smith,
Trade Register: Mannheim, HRB 432833, General Partner: John Wiley & Sons GmbH,
Location: Weinheim, Trade Register Mannheim, HRB 432296,
Managing Directors: Sabine Steinbach, Dr. Jon Walmsley

WILEY-VCH

Full Paper

xxxx

S. Sankaran, J. van Weerd, J. Voskuhl, M. Karperien, P. Jonkheijm* .....x–xx

Photoresponsive Cucurbit[8]uril-Mediated Adhesion of Bacteria on Supported Lipid Bilayers

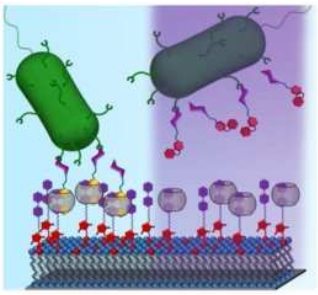

Specific *E.coli* binding and localized photoswitchable release are achieved using supramolecular chemistry, host–guest interactions, and supported lipid bilayers. In this study, ternary complexes of host molecule, cucurbit[8]uril, and a photoswitchable glycoconjugate guest, azobenzene-mannose form successfully on methyviologen-modified supported lipid bilayers. The proposed system with good nonfouling properties paves the way for the design of reusable biosensors that allow for dynamic presentation of bioactive ligands.

smll201502471(201502471)

small NANO MICRO

xxxx

Photoresponsive Cucurbit[8]uril-Mediated Adhesion of Bacteria on Supported Lipid Bilayers

*Shrikrishnan Sankaran, Jasper van Weerd, Jens Voskuhl, Marcel Karperien, and Pascal Jonkheijm**

ABSTRACT: In this work, the development of a photoresponsive platform for the presentation of bioactive ligands to study receptor–ligand interactions has been described. For this purpose, supramolecular host–guest chemistry and supported lipid bilayers (SLBs) have been combined in a microfluidic device. Quartz crystal microbalance with dissipation monitoring (QCM-D) studies on methyl viologen (MV)-functionalized oligo ethylene glycol-based self-assembled monolayers, gel and liquid-state SLBs have been compared for their nonfouling properties in the case of ConA. In combination with bacterial adhesion test, negligible nonspecific bacterial adhesion is observed only in the case of methyl-viologen-modified liquid-state SLBs. Therefore, liquid-state SLBs have been identified as most suitable for studying specific cell interactions when MV is incorporated as a guest on the surface. The photoswitchable supramolecular ternary complex is formed by assembling cucurbit[8]uril (CB[8]) and an azobenzene–mannose conjugate (Azo–Man) onto MV-functionalized liquid-state SLBs and the assembly process has been characterized using QCM-D and fluorescence techniques. Mannose has been found to enable binding of *E. coli* via cell-surface receptors on the nonfouling supramolecular SLBs. Optical switching of the azobenzene moiety allows us to "erase" the bioactive surface after bacterial binding, providing the potential to develop reusable sensors. Localized photorelease of bacterial cells has also been shown indicating the possibility of optically guiding cellular growth, migration, and intercellular interactions.

1. Introduction

Surface immobilization strategies of bioactive ligands such as peptides, carbohydrates, DNA, and proteins have enabled widespread development of functional surfaces for biomedical applications and studies.[1–4] Preliminary work in the field dealt with identifying biologically nonfouling components that could be deposited on surfaces and also chemically modified for the presentation of bioactive ligands. Some of the most successful strategies include self-assembled monolayers (SAMs),[5,6] polymeric networks,[7,8] hydrogels,[9] and supported lipid bilayers (SLBs).[10] Such surfaces have been used to develop biosensors for detection and diagnostics,[11,12] medical implant coatings,[13] platforms for studying cellular processes,[14] and tissue engineering.[15] However living entities predominantly exist in, interact with and modify a constantly changing environment. This led to the requirement for bioactive ligands to be presented in a highly dynamic manner to mimic the natural environment of eukaryotic and prokaryotic cells. Consequently, strategies are being developed to not only introduce such dynamic properties but also responsiveness, which is the ability to change some properties of the system in response to an external stimulus. Chemical, optical, and electrochemical stimuli-responsive systems enable us to study biological processes that are triggered by a

S. Sankaran, Dr. J. van Weerd, Dr. J. Voskuhl, Prof. P. Jonkheijm, Molecular Nanofabrication Group of the MESA+ Institute for Nanotechnology, Bioinspired Molecular Engineering Laboratory of the MIRA Institute for Biomedical Technology and Technical Medicine, University of Twente, P.O. Box 217 , 7500 AE Enschede, The Netherlands
Dr. J. van Weerd, Prof. M. Karperien, Developmental Bioengineering of MIRA Institute for Biomedical Technology and Technical Medicine, University of Twente, P.O. Box 217 7500 AE Enschede, The Netherlands
Correspondence to: Prof. P. Jonkheijm (E-mail: p.jonkheijm@utwente.nl)

Q1

10.1002/smll.201502471

change in the environment.[16,17] While traditional surface immobilization strategies allow for spatial control of bioactive ligands,[18] dynamics and responsiveness allow for temporal control of these ligands.[19,20]

In this light, SLBs have emerged as a powerful system for the development of a biomimetic surface since they are representative of the cell membrane. They can be used as model surfaces to study cell–ECM and cell–cell interactions.[21–24] Supramolecular chemistry has been successfully used in generation of several dynamic and responsive architectures by virtue of the reversible noncovalent forces involved in the self-assembly process.[25] By careful design and selection of the molecular components and the environment in which they interact, materials with novel properties can be developed. Host–guest systems have been especially successful towards the development of novel architectures for biomedical applications.[26] These systems have the advantage that they operate in an aqueous environment with micromolar affinities and with reasonable specificities. A few surface-confined molecular platforms have been developed using host molecules such as cyclodextrins and cucurbiturils for addressing living cells. Usually the host or guest molecule is anchored to the surface while its counterpart is conjugated to a bioactive ligand, allowing for dynamic and reversible presentation of ligands. Moreover, responsive presentation of ligands is made possible by competition with high affinity guests or a change in molecular properties such as, photoisomerization of azobenzenes,[19–23] and redox cycling of methyl viologen (MV) and ferrocene.[20–24] Modifications caused by such stimuli can change the guest molecule's affinity towards the host, causing it to either bind stronger or get expelled. A few SAM-based platforms have been recently developed that were able to address and manipulate cells. Preliminary reports of electro- and photoresponsive supramolecular surfaces for mammalian and bacterial cells have emerged in the last few years.[20,27–29] These reports highlight the promise of employing supramolecular chemistry to develop dynamic and responsive platforms to address living entities. However, further exploration and careful characterization of the surface assembly process are required to understand and improve various aspects of these systems, such as their non-fouling nature, cell adhesion effects, and localized responsiveness. In the present work, we attempt to address these issues by combining the versatility of supramolecular chemistry with the biomimetic nature of SLBs.

For the first time, we report the development of a supramolecular host–guest system incorporated on SLBs enabling the photoresponsive display of a bioactive ligand for the selective adhesion and release of living cells. To this end, bacterial adhesion to mannose was explored for several reasons. Uropathogenic *E. coli* initiates an infection by binding to mannose sugar molecules found in glycoproteins and glycolipids of the glycocalyx of target cells. This binding event is mediated by the FimH receptors on the bacterial Type1 pili and exhibits complex relations to the surface density of mannose and shear stress induced by the flow of bodily fluids.[30] Several strategies have been devised to study pathogen binding and develop suitable inhibitory molecules.[31–33] Still, novel platforms are required to understand pathogen binding and allow for the rapid detection of these pathogens in medical samples. Bacteria pose additional challenges in biosensing due to their small size, highly heterogeneous surface components, motility, and negatively charged cell surface causing nonspecific electrostatic interactions with surfaces. We carefully developed our platform to systematically address these issues.

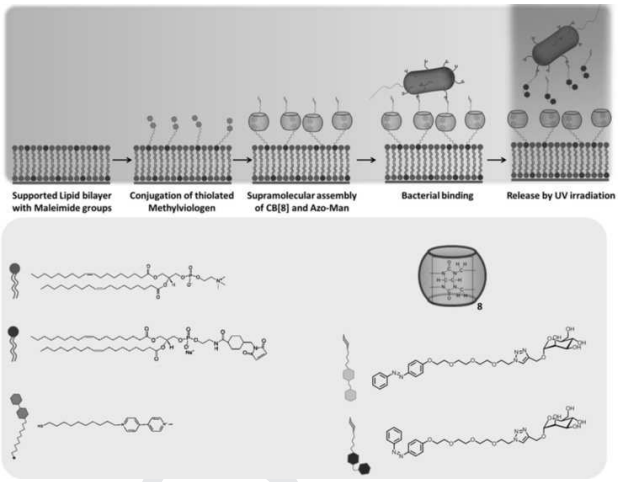

Scheme 1. Step-wise assembly and release scheme followed by chemical structures of the individual components used.

As shown in **Scheme 1**, we used liquid-state SLBs as the biomimetic background layer onto which we were able to assemble a ternary host–guest complex. First, the SLB was chemically modified with a thiolated methyl viologen (MV–SH). Second, MV acts as the first guest molecule that can bind within the cavity of cucurbit[8]uril (CB[8]), the supramolecular host molecule. CB[8] is a hollow pumpkin-shaped macrocylic host molecule made of 8 glycouril monomer units.[34] The cavity is hydrophobic and can accommodate aromatic guest molecules. The rims of the cavity consist of polar carbonyl groups, allowing for ion–dipole interactions with positively charged molecules such as MV. The cavity is also big enough to accommodate a second guest molecule such as azobenzene.[35] Azobenzene, in its *trans* form can form a stable ternary complex with CB[8] and MV. Third, for specific adhesion of *E. coli*, we conjugated the azobenzene to a mannose unit (Azo–Man) with a triethyleneglycol linker. Lastly, upon irradiation with 360 nm UV light, azobenzene photoisomerizes into the *cis* form. The *cis* form is sterically hindered to fit within the cavity of CB[8], causing the affinity to be drastically reduced and as a result azobenzene is expelled from the cavity. In this study, mannose-modified azobenzene was used to impart photoresponsiveness to the system. Here, bacterial cells can normally bind to the surface-anchored mannose units but on application of 360 nm UV light, the expulsion of *cis* Azo–Man from the CB[8] cavity causes the removal of the cell from the surface.

NANO MICRO small

2. Results and Discussion

2.1. Selection of a Nonfouling MV-Functionalized Layer

In order to construct a reusable supramolecular platform for binding and release of living cells, we first needed to select a background layer with two important properties: 1) the ability to chemically incorporate MV, the first guest molecule and 2) minimize nonspecific interaction of biolomolecules and cells to the surface. To this end, we tested three potential candidates: oligoethyleneglycol SAM, gel-state and liquid-state SLBs. We have previously reported a tetraethyleneglycol-based SAM for supramolecular manipulation of mammalian cells.[20,36] In this case, SAMs bearing maleimide groups[37] were used to tether a thiolated methyl viologen (MV-SH). The SAM was shown, to some extent, to be nonfouling and was used for mammalian cell binding and electrochemical release thereof.[36] Alternatively, we explored the use of model membranes in the form of SLBs. Such SLBs, pioneered by McConnell and co-workers, consist of a two-ply sheet of lipid molecules and can mimic natural cell membranes in terms of the lateral mobility of the lipids and associated ligands.[38,39] A relevant feature of SLBs is their inherent nonfouling nature. In the case of zwitterionic phosphocholine-based SLBs, negligible adsorption of various other naturally occurring proteins was observed.[40] This attribute of SLBs strongly influences cell adhesion kinetics and is able to prevent cells from adhering to its surface.[21] The chemical make-up of lipids, e.g., the saturation of acyl chains can have a profound effect on lipid lateral mobility and phase behavior of SLBs as a function of temperature. For example, the liquid-state (L_α phase) is characterized by a disordered packing of lipids due to the presence of unsaturated acyl chains, low melting temperature and high lipid lateral mobility, $>\mu m^2\ s^{-1}$. On the contrary, lipids with saturated acyl chains tend to pack more tightly in the gel-state (L_β phase), increasing their T_m and resulting in a reduced lateral mobility by at least one order of magnitude.[41] In addition, chemical modification of SLBs to alter its surface properties has been shown on various accounts.[22,42–44]

Although SLBs have been used in a multitude of cell studies, integrating them with supramolecular host–guest chemistry remains unexplored. Apart from their nonfouling nature, SLBs have the added advantage that they mimic the natural environment of eukaryotic cell membranes. In this study, we integrated liquid- and gel-state SLBs with supramolecular chemistry. All three aforementioned methods offered the possibility to form tightly packed layers of MV at well-defined surface densities.

We first evaluated the nonfouling nature of these types of MV-functionalized surfaces, i.e., SAM, liquid- and gel-state SLBs, towards biomolecules such as proteins and cells. Since MV carries a double-positive charge, electrostatic interactions could potentially cause nonspecific interactions with biomolecules despite the nonfouling nature of the background layer. MV-functionalized ethyleneglycol-based SAMs on gold were made as reported previously.[36] We followed the formation of gel-state and liquid-state SLBs doped with PE-MCC (maleimide-containing lipid) on SiO_2 surfaces using QCM-D. In both cases, we were able to observe the conjugation of MV–SH onto these SLBs (Figure S1, Supporting Information). In all cases, a 1% surface density of MV was readily obtained. Since we wanted to develop a system for bacterial binding to glycoconjugates, we chose to test the resistance of our modified surfaces against a mannose-binding lectin, Conconavalin A (ConA).

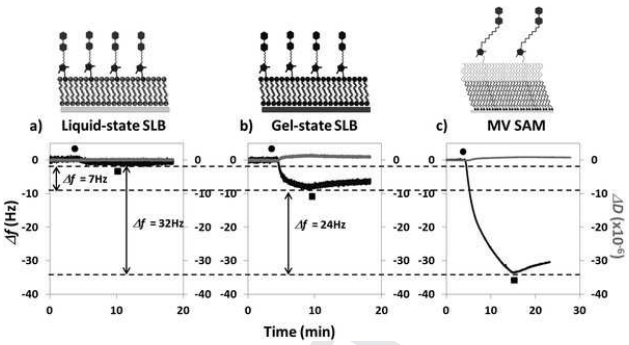

Figure 1. QCM-D response plots to flowing 1×10^{-6} m ConA (·) over a) a liquid-state SLB, b) a gel-state SLB, and c) an oligoethylenegylcol-based SAM, each with 1% surface density of MV followed by rinsing with buffer (■). Change in frequency (Δf, black) and dissipation (ΔD, gray) values correspond to the fifth overtone.

From **Figure 1**, we clearly observed that the liquid-state SLB was the most nonfouling of the three surfaces when incubated with 1×10^{-6} M ConA. The nonfouling nature of SLBs behavior is often ascribed to the neutrally charged PC head-group in a large pH range, $3 < pH < 10$. In addition, PC is known to attract a water layer that hampers the adsorption of proteins. In the case of liquid-state SLBs, the high lateral mobility of PC lipids further favors this protein repellent property.[40] It has been proposed that out-of-plane z-axis mobility of liquid-state SLB results in undulatory motions of the bilayer that further interferes in cell and protein binding.[45] Similar to SAMs, gel-state SLBs and their constituents exhibit nearly no lateral mobility. Despite the absence of such out-of-plane mobility in gel-state SLBs, nonspecific binding of ConA was significantly less compared to MV–SAMs. This difference can be ascribed to the fact that zwitterionic gel-state SLBs do however, to some extent, retain nonfouling properties. Previous QCM-D analysis of gel-state SLBs in the presence of serum showed negligible protein fouling on such surfaces.[23] In addition, a cell adhesion study performed on polymerized zwitterionic SLBs consisting of Bis-SorbPC showed a high degree of cell repellence towards murine-derived macrophages despite the absence of lipid lateral mobility.[46]

Clearly, significant fouling was observed on gel-state SLBs and SAM PEG layers, whereas on the liquid-state SLB no fouling was observed in the case of nonspecific adhesion of ConA. To further confirm that using methyl-viologen-functionalized gel-state SLBs and methyl-viologen-modified

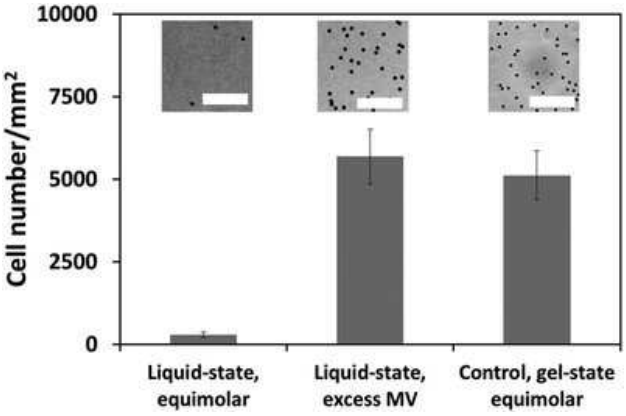

Figure 2. Nonspecific bacterial adhesion to three lipid bilayers that were presenting methyl viologen. Liquid-state and gel-state SLBs were made of using positively (MV-PEMCC) and negatively (TR-DHPE) charged lipid constituents in an equimolar amount 0.1%. Liquid-state SLB using 1% MV-PEMCC and 0.1% TR-DHPE was also made and used. Bacterial cells have been falsely colored black for better visualization. Data presented as mean ± STD, $n = 4$. Insets are sample images of the respective surfaces.

SAM PEG-based layers, leads to significant nonspecific adhesion of bacterial cells to these surface exceeding by far that observed on the methyl-viologen-functionalized liquid-state SLB, we performed bacterial adhesion tests on these three layers.

Figure 2 shows data of a nonspecific bacterial adhesion test on a liquid-state SLB with two ratios of positively (methyl viologen-PEMCC) and negatively (TR-DHPE) charged lipid constituents. On liquid-state SLBs made of an 0.1% ratio of positively and negatively charged constituents, negligible nonspecific bacterial adhesion was observed. This observation is in strong contrast with the considerable nonspecific bacterial adhesion observed on liquid-state SLBs made of a lipid mixture with an excess of positively charged MV and, also, with gel-state SLBs made of an equimolar amount of viologen-PEMCC and TR-DHPE. Based on these data, we confirm that the balance of positive and negative charges on the layer is of utmost importance to prevent fouling of the surface by the bacteria through nonspecific electrostatic interactions. We were not able to find a condition on a gel-state SLB where bacteria do not adhere.

Subsequently, we attached MV to the maleimide-modified SAM PEG system (Figure 1c). We incubated the MV with host CB[8], and with a mixture of CB[8] and second guest azobenzene-modified mannose. We monitored bacterial adhesion to these four layers (Figure S2, Supporting Information). Clearly, and as expected, the SAM with maleimide functional groups is preventing nonspecific interactions with the bacteria. However, the introduction of MV on the SAM resulted, also as expected, in substantial nonspecific electrostatic interactions with the bacteria, to a similar extent as observed in the case of methyl-viologen-functionalized gel-state SLBs in Figure 2. While the bacterial adhesion on the SAM including the biospecific mannose ligands only showed a small increase in the number of adhered bacteria, performing bacteria adhesion and subsequent photocontrolled release experiments on these types of SAMs seems redundant. Then, we attempted to find a condition on a SAM PEG-based surface where such nonspecific interactions would be suppressed. To this end, we reacted the maleimide-functionalized SAMs with a mixture of thiol-functionalized MV and 3-mercapto-1-propane sulfonate (MPS), which can provide negative charges to balance the positive charges given by the incorporation of MV on the SAM. We prepared different SAMs using various ratios of these two compounds. Bacteria adhered to all of these SAMs (Figure S3, Supporting Information). The adhered bacteria per area in the condition of MV and MPS used in a 1:3 ratio are still exceeding by large the nonspecific bacterial adhesion observed on MV-modified liquid-state SLB made of an equimolar ratio of MV and TR-DHPE. Taken together, MV-functionalized liquid-state SLBs were chosen to evaluate supramolecular ternary-complex formation, selective bacterial adhesion experiments, and subsequent studies for photoswitchable release of adhered bacteria.

For in situ monitoring of the SLB quality during various modification steps, a fluorescent lipid-dye conjugate, Texas Red-DHPE (TR-DHPE), was included at low doping densities. A typical characterization experiment for liquid-state SLBs involves monitoring of the rate of fluorescence recovery after the SLB that has been locally bleached. Such a fluorescence recovery after photobleaching (FRAP) experiment can provide insights into lipid lateral mobility. Successful formation of a defect free MV-modified (liquid-state) SLB was confirmed by observing uniform fluorescence in agreement with the observations made using QCM-D. This was further complemented by the deduced diffusion coefficients, which are well within the expected range for liquid-state SLBs, i.e., 0.95 μm s^{-1}. Texas Red-DHPE was used to monitor in situ further SLB modifications (see Section 2.2.2.).

2.2. Incorporating Supramolecular Components

2.2.1. QCM-D-Based Analysis

After having established a nonfouling layer grafted with MV, the self-assembly of the supramolecular host–guest complex was attempted. QCM-D was used to monitor the formation of the ternary complex on the MV–SLB. In **Figure 3**a, interaction and binding of CB[8] are observed, as indicated by a shift in frequency and dissipation. Subsequently, a titration of Azo–Man was performed from 20×10^{-6} M to 1×10^{-3} M in the presence of 100×10^{-6} M CB[8] to ensure that the equilibrium is driven towards complex formation. Concentration-dependent frequency and dissipation changes were clearly observed. Washing with only CB[8] after the titration caused dissociation of the Azo–Man and further washing with MilliQ water caused gradual dissociation of the complex. Changes in both dissipation and frequency values normally indicate that the adsorbed entities have viscoelastic properties. From

NANO MICRO small

the ΔD vs. Δf plot in Figure 3b, we witness a nearly linear relationship between the dissipation and frequency during the entire titration. This indicated that both the shifts in dissipation and frequency directly correlated to the amount of Azo–Man that was binding to the surface. When the saturation values corresponding to each Azo–Man concentration were plotted against the concentration, we obtained a similar Langmuir adsorption trend from both the frequency and dissipation values. Fitting to a Langmuir adsorption equation, yielded a dissociation constant (K_d) of $\approx 300 \times 10^{-6}$ M. This value is within an expected range for such supramolecular interactions but is higher than that previously reported by Scherman and co-workers ($\approx 70 \times 10^{-6}$ M) for CB[8] binding with azobenzenes in solution.[35] Most likely, the surface density of MV in our system is below what is required for maximum packing of CB[8] on the surface. The interligand spacing of MV molecules was estimated to be roughly 19 nm, calculated based on the method described by Tanaka and co-workers.[24] However, the outer diameter of cucurbit[8]uril has been reported to be only 1.75nm,[47] nearly a tenth of the MV interligand spacing. Finally, the bioactivity of the self-assembled ternary complex was confirmed through the specific binding of ConA with mannose on the second guest Azo–Man. ConA specifically adhered to a liquid-state SLB modified with supramolecularly assembled Azo–Man (Figure 3d) when compared to the bare MV-functionalized SLB (Figure 1a).

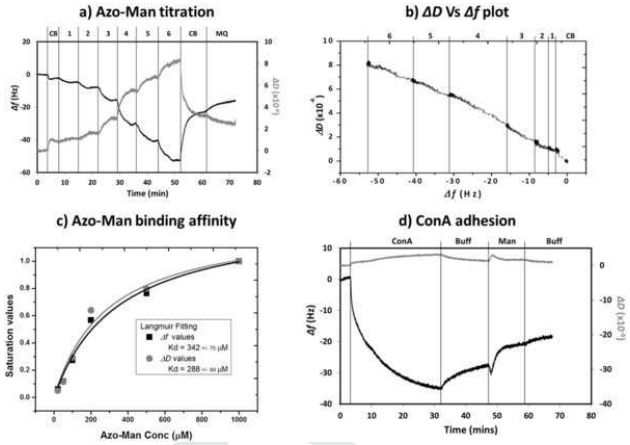

Figure 3. QCM-D analysis of the supramolecular assembly on liquid-state SLBs. The captions on top of the plots represent the different solutions used during the QCM-D measurement. a) Binding of CB[8] (CB) to an MV-functionalized SLB followed by titration of different concentrations of Azo–Man (1– 20×10^{-6} m, 2–50×10^{-6} m, 3–100×10^{-6} m, 4–200×10^{-6} m, 5–500×10^{-6} m, 6–1000×10^{-6} m) followed by washing with CB[8] and MilliQ water (MQ). All the Azo–Man solutions also contained 100×10^{-6} m CB[8]. b) ΔD vs. Δf plot for the Azo–Man titration part of Figure 3a. All captions above the plot are the same as in Figure 3a. c) Langmuir adsorption equation fitting of the saturation values from the frequency and dissipation changes seen during the Azo–Man titration. d) Adhesion of 1×10^{-6} m ConA onto CB[8]–Azo–Man-functionalized SLB followed by washing with HEPES NaCl buffer (Buff) and 10×10^{-6} m Mannose (Man). Change in frequency (Δf, black) and dissipation (ΔD, gray) values correspond to the fifth overtone.

2.2.2. Fluorescence-Based Analysis

As mentioned previously, TR-DHPE is usually used in SLBs to evaluate the quality and fluidity of the SLB, however it can also be used to monitor modification of the SLB in situ. This lipid–dye conjugate is usually synthesized by reacting the amine of a phosphatidylethanolamine lipid with the lower aromatic ring of Texas Red sulfonyl chloride, which resides at either the *ortho*- or *para*-positions,[48] resulting in an isomeric mixture. Interestingly, the fluorescence intensity of the *ortho* isomer has been shown to be pH dependent,[49] with lower intensities under basic conditions. Next to inspecting SLB integrity and approximate lipid lateral diffusion (vide infra), this property allowed us to track the MV reaction with the surface in time. The presence of the highly positively charged MV attracts hydroxide ion from the water and creates a local pH increase. As expected, we always observed a drop in the Texas Red fluorescence intensity when MV–SH was conjugated to the SLB (**Figure 4**a). To ensure that this was purely a surface chemistry effect, we checked the fluorescence intensity drop after addition of an unreactive MV. In this case, no significant drop in the intensity was observed (Figure 4a). Following this, we measured the changes in fluorescence intensities as the supramolecular components were assembled. When CB[8] bounds to the surface-immobilized MV, a slight rise in the fluorescence intensity was observed possibly due to the partial shielding of the charges of MV. When titrating with different concentrations of Azo–Man, the fluorescence intensity seems to drop at higher concentrations and seems to follow a similar trend as the binding curve in Figure 3c. The drop in fluorescence might be due to a change in local pH. Also, as seen in the FRAP experiment, increased Azo–Man concentrations causes the lateral mobility to reduce, which suggests crowding of the TR-DHPE lipid resulting in self-quenching. Nonetheless, the observed trend seems to follow the binding curve presented in Figure 3c. Furthermore, FRAP was used to study the attachment of MV to the SLB and the effect of the formation of the ternary complex on the lipid lateral mobility and diffusion coefficient (Figure 4c). In line with the trends observed in Figure 3a,b, the diffusion coefficient dropped after attachment of MV, increased on CB[8] adhesion and reduced again in the presence of increasing concentrations of Azo–Man. We tentatively interpret these observations as follows. Positively charged MV-lipids can possibly interact with negatively charged TR-DHPE resulting in its mobility drop. Subsequently, the binding of CB[8] causes shielding of MV allowing TR-DHPE to diffuse more freely in the bilayer. Further binding of increasing amounts of Azo–Man to the MV–CB[8] complex causes a drop in lateral mobility, probably since mannose, being highly hydrated, causes a crowding effect at the surface. This observed trend also seems to follow the binding

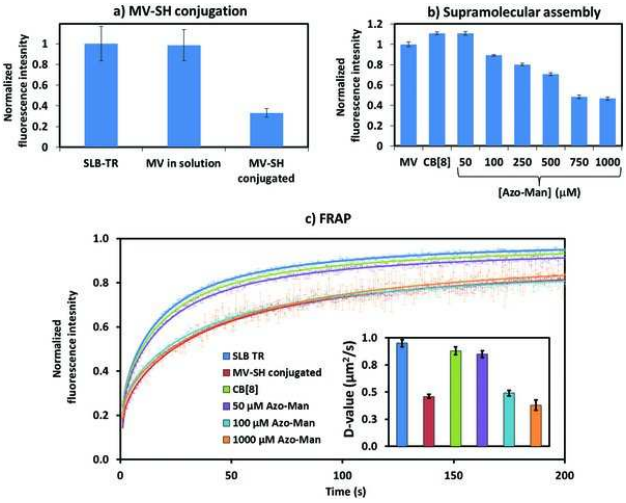

Figure 4. Fluorescence-based analysis of the supramolecular SLBs. a) Drop in fluorescence intensity of TR-DHPE due to the conjugation of MV–SH with PE-MCC lipids in the SLB. All intensities have been normalized to the fluorescence due to TR in the SLB before MV–SH conjugation. b) Change in the fluorescence intensities seen during assembly of the CB[8] and Azo–Man. All Azo–Man solutions in the titration also contained 100×10^{-6} m CB[8]. Intensity values have been normalized to the fluorescence due to TR in the SLB after MV–SH conjugation. c) FRAP analysis of the supramolecular assembly on the surface. Inset plot represents diffusion coefficients. The colors in the legend apply for both the fluorescence recovery curves and the diffusion coefficient plot. Data presented as mean ± STD, $n = 2$.

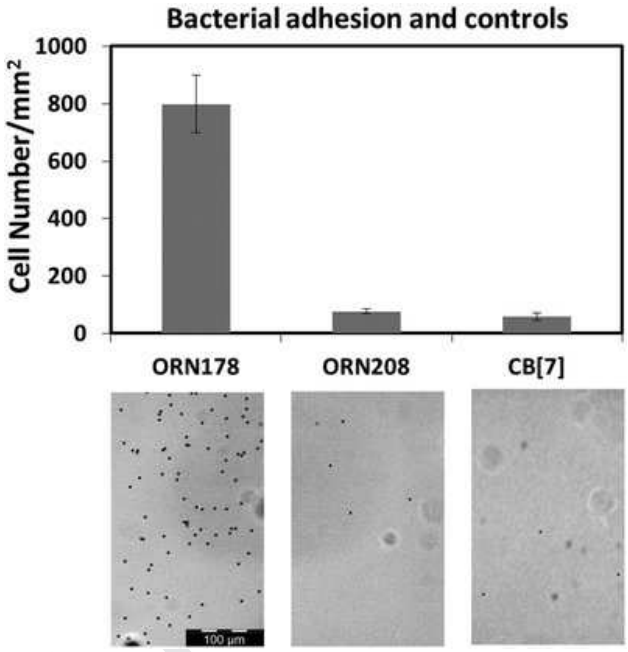

Figure 5. Number of bacterial cells immobilized on supramolecular SLBs. For ORN178 and ORN208 adhesion experiments, 0.1 O.D.$_{600nm}$ of the bacteria along with 10×10^{-6} m CB[8] and 100×10^{-6} m Azo–Man in buffer was used. For the adhesion test of ORN178 to supramolecular SLBs containing CB[7], 0.1 O.D.$_{600nm}$ of the bacterial solution with 10×10^{-6} m CB[7] and 100×10^{-6} m Azo–Man was used. Data presented as mean ± STD, $n = 6$. Bacterial cells in the images have been falsely colored black to improve visualization.

curve presented in Figure 3c. These results highlight the use of TR-DHPE for in situ monitoring of the MV reaction and assembly of the supramolecular host–guest complex.

2.3. Bacterial Capture and Release

2.3.1. Bacterial Adhesion and Controls

Confident that the supramolecular assembly of CB[8] and Azo–Man is possible on liquid-state SLBs, we proceeded to test bacterial adhesion onto these surfaces in microfluidic channels. For this purpose, we chose to use the ORN178 and ORN208 bacterial strains.[50] ORN178 is an *E. coli* K12 derivative expressing a native version of the FimH receptor, allowing it to specifically bind mannose. ORN208 has a genetically modified FimH receptor with a single-point mutation and is unable to bind mannose. Apart from this, both strains are identical. When the supramolecular surface was exposed to ORN178, bacterial cells were seen adhering to the surface and did not dissociate even in the presence of strong flow (300 μL min^{-1}) (**Figure 5**). To ensure that the bacterial cells had adhered specifically to thesupramoelcularly mannose units in the host–guest system, two control experiments were performed. First, adhesion of ORN208 was tested and we observed that even at a lower flow speed (15 μL min^{-1}), only a negligible number of cells were visible at the surface (Figure 5). Similarly, when CB[7] was used instead of CB[8] only MV was able to occupy the smaller cavity of CB[7] resulting in almost no ORN178 cells (less than 5% compared to the ternary complex) adhering to the surface (Figure 5). These experiments confirmed that bacterial adhesion was specific to the mannose presented in a supramolecular fashion using the ternary host–guest complex on SLBs. We also confirmed that CB[8] and Azo–Man do not affect bacterial viability by testing their growth on agar plates after being mixed together for an hour. The presence of CB[8] and Azo–Man did not reduce the number of bacterial colonies seen compared to the control (Figure S4, Supporting Information). In addition, UV exposure for 5 min did not reduce the number of bacterial colonies compared to the control (Figure S5, Supporting Information).

2.3.2. Bacterial Release Due to Azo–Man Photoisomerization

Next, we tested whether the photoisomerization of Azo–Man under UV irradiation could cause the dissociation of the bacterial cells from the surface. For this purpose, we first al-

NANO MICRO small

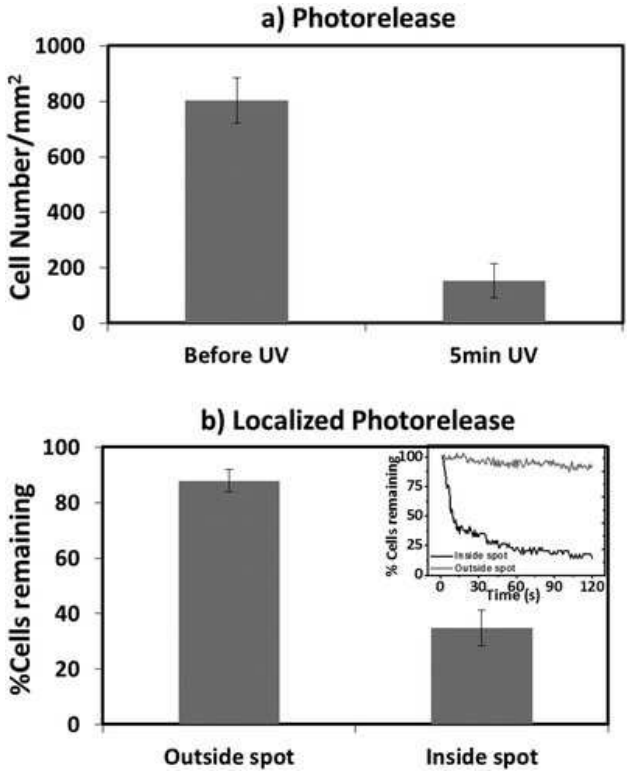

Figure 6. Plots representing results from bacterial release experiments by irradiation of 360 nm UV light in the presence of 300 μL min^{-1} flow. a) Before UV irradiation, cell detachment was not observed even in the presence of flow whereas 5 min UV irradiation caused detachment of nearly 80% of the cells. Error bars obtained from three individual release experiments. b) Localized photorelease was performed by irradiating the surface with UV light from the microscope lens using a field diaphragm. The columns represent percentage of cells remaining inside or outside the irradiated spot after 4 min irradiation. Error bars were obtained from two experiments with localized release done on three individual spots each. Inset represents the detachment of bacterial cells inside (black line) and outside (gray line) the irradiated spot as a function of time.

lowed ORN178 cells to adhere to the supramolecular SLB and then irradiated the surface with 360 nm UV light. At 300 μL min^{-1} in the presence of UV irradiation, we observed rapid detachment of bacterial cells from the surface (**Figure 6**a). Interestingly, at flow speeds of 100 μL min^{-1} and 200 μL min^{-1}, rapid dissociation was not observed. This could possibly be explained by the fact that the photoisomerization of azo-benzenes has only around 75%–80% efficiency.[19] Since *E. coli* typically produces a few hundred FimH receptors, stronger multivalent binding to several Azo–Man units is expected. Therefore higher flow speeds are needed to overcome the overall interaction strength of the remaining bound FimH and Azo–Man bonds.

Furthermore, we tested whether it would be possible to selectively release bacterial cells from a well-defined region by localized UV irradiation. Local UV irradiation was achieved by closing the field diaphragm and illuminating with 360 nm UV light. At a flow of 300 μL min^{-1}, bacterial cells were seen detaching from the irradiated spot, while the vast majority of cells outside this spot remained bound (Figure 6b). This even occurred with simultaneous illumination with white light. This enabled real-time imaging of the photorelease as shown by the plot in the inset of Figure 6b (Video S1, Supporting Information). The photorelease seemed to occur rapidly within the irradiated spot while bacterial cells outside the spot seemed to stay immobilized during this period. This confirmed that localized release of immobilized bacterial cells can be easily achieved with this photoresponsive supramolecular system.

3. Conclusion

We have successfully demonstrated for the first time the combination of supramolecular host–guest chemistry and SLBs to develop photoresponsive supramolecular SLBs. Comparisons with other similarly possible supramolecular surfaces on SAMs and gel-state lipid bilayers indicated that liquid-state lipid bilayers were the most suitable for specific bacterial adhesion. Each step in the molecular construction of the system, including SLB formation, conjugation of the first guest, supramolecular assembly of host–guest components and photorelease have been carefully characterized using QCM-D measurements, fluorescence, and bright-field microscopy. Using the photoisomerizable glycoconjugate, Azo–Man, the system has been validated for bacterial binding and release. Interesting aspects of the system including the ability to quickly monitor supramolecular assembly through fluorescence intensity changes, requirement of a certain shear stress provided by flow for bacterial photorelease and localized photorelease have been investigated. The system can potentially be used to develop reusable biosensor chips where the detection of specific pathogenic strains in a sample can be performed by capture to the surface followed by photorelease, allowing for detection in a fresh sample to be performed. Further, localized release would enable photo patterning or photo guiding of cells on the surface enabling the study of growth, migration, and intercellular interactions.

4. Experimental Section

Materials: All starting materials and chemicals were purchased from Sigma–Aldrich, Fluka, Serva, Becton Dickinson, Avanti Polar Lipids, Microchem, Thermo Fisher, Invitrogen, and Acros organics, and they were used as received, unless otherwise stated. MV–SH was synthesized as previously reported in literature.[51] The Azo–Man glycoconjugate was also synthesized as previously reported in literature.[19] Both ORN178 and ORN208 bacterial strains were kindly provided

by Prof. Luc Brunsveld, TU/e. MilliQ water with a resistivity higher than 18 MΩ cm^{-1} was used in all experiments.

QCM-D: Thiolated ethyleneglycol-based SAMs bearing maleimide groups were formed on gold QCM resonators (Q-Sense) as described elsewhere.[36] SLBs were formed on SiO_2 QCM resonators (Q-Sense). Prior to use, the resonators were cleaned with ethanol, water, and with 30 min UV-ozone treatment (UV/Ozone Procleaner plus, Bioforce Nanosciences). After mounting the cleaned resonators in the QCM-D holder, degassed 5×10^{-3} M PBS (Sigma–Aldrich, pH 7.4) was initially flowed. After obtaining a stable baseline (less than Δ 0.5 Hz during 10 min), 0.5 mg mL^{-1} large unilamellar vesicles (LUVs) were flown through the device. The 1 mg mL^{-1} stock LUV solution in milliQ was diluted 1:1 with 10×10^{-3} M PBS (Sigma–Aldrich, pH 7.4) just before vesicle addition. For liquid-state SLBs, these steps were performed at 22 °C and for gel-state SLBs, the temperature was raised to 45 °C. All subsequent measurements were performed at 22 °C. Subsequently, 50×10^{-3} M sodium phosphate buffer (pH 6.8) was passed through until a stable baseline was reached. A freshly prepared 1×10^{-3} M MV–SH solution in 50×10^{-3} M sodium phosphate buffer (pH 6.8) was flowed in the chamber and allowed to react for 1 h. Assembly of the ternary complex of CB[8] and Azo–Man was performed in MilliQ water using concentrations mentioned in the main text. A 1×10^{-6} M Concanavalin A (ConA) solution in buffer (10×10^{-3} M HEPES, 137×10^{-3} M NaCl, 1×10^{-3} M $MnCl_2$, 1×10^{-3} M $CaCl_2$, pH 7.0) was flown through the device to monitor nonspecific and specific binding. All fluids were exchanged continuously at 100 μL min^{-1} using a peristaltic pump.

PDMS Flow Channel: A silicon flow channel master was produced by standard photolithography steps and deep reactive ion etching. The polydimethylsiloxane (PDMS) flow channels were prepared from a degassed mixture of 10:1 Sylgard 184 elastomer and curing agent (Dow Corning Corp), which was casted onto the silicon master and cured at 80 °C for 1 h. The flow channels were cut to size and inlets and outlets were punched using a 1 mm Ø punch (Harris Uni-core; Sigma–Aldrich). The single straight channel had a width of 1.5 mm and a height of 50 μm.

PDMS Bonding: Standard glass microscope slides (Menzel-Gläser) were rinsed and sonicated extensively with acetone, ethanol, and MilliQ water, and dried prior to UV-ozone exposure (UV/Ozone Procleaner plus, Bioforce Nanosciences) for at least 20 min. After UV exposure, the microscope slides were rinsed with ethanol, water, and dried under a stream of nitrogen. Both cut-out PDMS flow channels and cleaned microscope slides were treated with oxygen plasma for 30 s at 40 W (Plasma prep II, SPI supplies) after which they were bonded immediately. The chips were placed on a hot plate for 10 min at 70 °C to increase the binding strength. Tygon tubing (VWR, 0.25 mm inner Ø and 0.76 mm outer Ø) was inserted into the PDMS. The assembled μSLB flow channels were placed in an oven at 60 °C for 1 h. Leak-free operation was seen for flow rates up to 2 mL min^{-1}.

Vesicle Preparation: 1,2-Dioleoyl-sn-glycero-3-phosphocholine (DOPC, Avanti Polar Lipids) was stored as a 10 mg mL^{-1} stock solution in chloroform at −20 °C and used as the main constituent in liquid-state SLBs. 1-Myristoyl-2-palmitoyl-*sn*-glycero-3-phosphocholine (MPPC, Avanti Polar Lipids) was stored as a 10 mg mL^{-1} stock in chloroform at −20 °C and used as the major constituent for gel-state SLBs. 1,2-Dipalmitoyl-sn-glycero-3-phosphoethanolamine-N-[4-(p-maleimidomethyl)cyclohexane-carboxamide] (PE-MCC, Avanti Polar Lipids) was stored as a 2 mg mL^{-1} stock in chloroform at −20 °C. The charged lipid–dye conjugate, Texas Red-1,2-dihexadecanoyl-sn-glycero-3-phosphoethanolamine (TR-DHPE, Invitrogen) was stored as a 1 mg mL^{-1} stock solution in methanol at −20 °C. Desired molar ratios of the DOPC/MPPC, PE-MCC, and TR-DHPE were mixed and dried under a flow of nitrogen in a glass vial, and subsequently placed under vacuum overnight. The resulting lipid film was resuspended by vortexing in MilliQ water to form multilamellar vesicles (MLVs) at 1 mg mL^{-1}. The MLV solution was extruded 11 times through a 100 nm polycarbonate membrane (Avanti Polar Lipids). The resulting large unilamellar vesicles (LUVs) were kept at room temperature and used within 2 weeks. For liquid-state SLBs, all these steps were performed at room temperature and for the gel-state SLBs, they were performed at 60 °C.

Supramolecular SLB Formation: SLB formation was achieved by dilution of the LUV solution to 0.5 mg mL^{-1} in 10×10^{-3} M PBS pH 7.4 (Gibco, lacking $MgCl_2$ and $CaCl_2$). Prior to LUV incubation, the channels were flushed briefly with 10×10^{-3} M PBS. The channels were then incubated with the vesicle suspension for at least 30 min to allow for vesicle adsorption and rupture to occur. For gel-state SLBs, this step was performed at 60 °C. Subsequently, the chips were washed with an excess of MilliQ water (300 μL min^{-1}). From this point forth, care was taken to ensure that no air bubbles entered the device. Coupling of MV–SH to the PE-MCC units in the SLB was done by passing 300 μL of 1×10^{-3} M MV–SH in 50×10^{-3} M sodium phosphate buffer (pH 6.8) at 300 μL min^{-1} through the channel and allowing it to incubate for 1 h. Further assembly of CB[8] and Azo–Man was performed by passing 200–300 μL of each solution, as indicated in the main text, at 300 μL min^{-1} and allowing it to incubate in the channel for 10 min unless stated otherwise. Experiments were done by first assembling all components and monitoring the adhesion and photorelease of bacteria and subsequently the complete supramolecular SLB was reinstalled for a new experiment. We have not quantified how often this process can be done.

Fluorescence Microscopy: An Olympus inverted IX71 epifluorescence research microscope with a Xenon X-cite 120PC as a light source and a digital Olympus DR70 camera for image acquisition was used to acquire fluorescence micrographs of the TR-DHPE in the SLBs. To this end, green excitation ($510 \leq \lambda_{ex} \leq 550$ nm) and red emission ($\lambda_{em} > 590$ nm) was filtered using the U-MWG2 Olympus filter cube. To image the FRET gradient, UV excitation ($325 \leq \lambda_{ex} \leq 375$ nm) and broad emission ($\lambda_{em} > 420$ nm) were filtered. Bacterial ad-

NANO MICRO small

hesion was imaged using top bright-field illumination. In all instances, ISO200 camera settings were used to record high quality, low noise images. In the case of fluorescence micrographs, care was taken to ensure image acquisition that was performed in the linear response regime. For photoisomerization experiments, a filter cube with excitation of 350–360 nm was used with maximum illumination intensity. Localized release experiments were performed by closing the field diaphragm in the UV excitation path (epi). Brigth-field illumination enabled real-time image acquisition.

Fluorescence Recovery After Photobleaching: FRAP measurements were conducted using a Nikon A1 CSLM with a 20× objective. To derive the diffusion coefficient, modified Bessel functions as described by Soumpasis et al. 1983 were used. Data were corrected for acquisition bleaching and normalized. FRAP data were analyzed with FRAPAnalyser (University of Luxembourg).

Bacterial Cell Culture: The bacterial strains ORN178 and ORN208 were grown overnight in LB media using tetracycline as the selective antibiotic. These were then spun down at 5000 g for 10 min and the supernatant was discarded. The bacteria were washed twice with 10×10^{-3} M HEPES, 137×10^{-3} M NaCl, pH 7 buffer by centrifugation and resuspension. Finally the bacteria were reconstituted in this buffer and their optical density at 600 nm was measured.

Bacterial Adhesion: OD 0.1 solutions in buffer (10×10^{-3} M HEPES, 137×10^{-3} M NaCl, pH 7.0) were prepared of ORN178 and ORN208. Prior to flowing, the bacteria through the device, $MnCl_2$ and $CaCl_2$ were added at final concentrations of 1×10^{-3} M each. 200 μL of bacterial solution was flown through the chip at 300 μL min^{-1}. The flow was stopped and the cells were left to settle for 15 min. After the set incubation period, flow was applied as indicated in the main text.

Data Analysis: Image processing was performed using ImageJ (NIH) and the obtained data were analyzed and plotted using Origin (OriginLab) and Excel (Microsoft).

Supporting Information

Supporting Information is available from the Wiley Online Library or from the author.

Acknowledgements

S.S. and J.v.W. contributed equally to this work. S. Sankaran, J. Voskuhl, and P. Jonkheijm acknowledge the European Research Council for Starters Grant Sumoman 259183 and Proof of Concept BioStealth 31015. Dr. Jasper van Weerd, Marcel Karperien, and Pascal Jonkheijm thank NanoNextNL (program 6C11).

Received: August 17, 2015
Revised: MM DD, YYYY
Published Online: MM DD, YYYY

[1] G. Henderson, M. Bradley, *Protein Technol. Syst. Biol.* **2007**, *18*, 326.
[2] C. D. Rillahan, J. C. Paulson, *Annu. Rev. Biochem.* **2011**, *80*, 797.
[3] V. Trevino, F. Falciani, H. A. Barrera-Saldaña, *Mol. Med.* **2007**, *13*, 527.
[4] P. Jonkheijm, D. Weinrich, H. Schröder, C. M. Niemeyer, H. Waldmann, *Angew. Chem. Int. Ed.* **2008**, *47*, 9618.
[5] K. L. Prime, G. M. Whitesides, *J. Am. Chem. Soc.* **1993**, *115*, 10714.
[6] B. T. Houseman, E. S. Gawalt, M. Mrksich, *Langmuir* **2003**, *19*, 1522.
[7] M. Krishnamoorthy, S. Hakobyan, M. Ramstedt, J. E. Gautrot, *Chem. Rev.* **2014**, *114*, 10976.
[8] G. L. Kenausis, J. Vörös, D. L. Elbert, N. Huang, R. Hofer, L. Ruiz-Taylor, M. Textor, J. A. Hubbell, N. D. Spencer, *J. Phys. Chem. B* **2000**, *104*, 3298.
[9] P. Y. W. Dankers, M. J. A. van Luyn, A. Huizinga-van der Vlag, G. M. L. van Gemert, A. H. Petersen, E. W. Meijer, H. M. Janssen, A. W. Bosman, E. R. Popa, *Biomaterials* **2012**, *33*, 5144.
[10] E. T. Castellana, P. S. Cremer, *Surf. Sci. Rep.* **2006**, *61*, 429.
[11] X. D. Hoa, A. G. Kirk, M. Tabrizian, *Biosens. Bioelectron.* **2007**, *23*, 151.
[12] N. J. Ronkainen, H. B. Halsall, W. R. Heineman, *Chem. Soc. Rev.* **2010**, *39*, 1747.
[13] D. Campoccia, L. Montanaro, C. R. Arciola, *Biomaterials* **2013**, *34*, 8533.
[14] M. Mrksich, *Chem. Soc. Rev.* **2000**, *29*, 267.
[15] R. Langer, *Acc. Chem. Res.* **2000**, *33*, 94.
[16] a) J. Brinkmann, E. Cavatorta, S. Sankaran, B. Schmidt, J. van Weerd, P. Jonkheijm, *Chem. Soc. Rev.* **2014**, *43*, 4449; b) B. Chang, M. Zhang, G. Qing, T. Sun, *Small* **2015**, *11*, 1097; c) J. Boekhoven, S. I. Stupp, *Adv. Mater.* **2014**, *26*, 1642; d) H. Yang, B. Yuan, X. Zhang, O. A. Scherman, *Acc. Chem. Res.* **2014**, *47*, 2106.
[17] a) C. G. Sanchez, Q. Su, H. Schönherr, M. Grininger, G. Nöll, *ACS Nano* **2015**, *9*, 3491; b) G. Pan, B. Guo, Y. Ma, W. Cui, F. He, B. Li, H. Yang, K. J. Shea, *J. Am. Chem. Soc.* **2014**, *136*, 6203.
[18] J. Voskuhl, J. Brinkmann, P. Jonkheijm, *Curr. Opin. Chem. Biol.* **2014**, *18*, 1.
[19] J. Voskuhl, S. Sankaran, P. Jonkheijm, *Chem. Commun.* **2014**, *50*, 15144.
[20] Q. An, J. Brinkmann, J. Huskens, S. Krabbenborg, J. de Boer, P. Jonkheijm, *Angew. Chem. Int. Ed.* **2012**, *51*, 12233.
[21] A. S. Andersson, K. Glasmastar, D. Sutherland, U. Lidberg, B. Kasemo, *J. Biomed. Mater. Res. A* **2003**, *64A*, 622.
[22] S. Svedhem, D. Dahlborg, J. Ekeroth, J. Kelly, F. Hook, J. Gold, *Langmuir* **2003**, *19*, 6730.
[23] M. Andreasson-Ochsner, G. Romano, M. Hakanson, M. L. Smith, D. E. Leckband, M. Textor, E. Reimhult, *Lab Chip* **2011**, *11*, 2876.
[24] A. Körner, C. Deichmann, F. F. Rossetti, A. Köhler, O. V. Konovalov, D. Wedlich, M. Tanaka, *PLoS One* **2013**, *8*, e54749.
[25] X. Yan, F. Wang, B. Zheng, F. Huang, *Chem. Soc. Rev.* **2012**, *41*, 6042.
[26] H. Yang, B. Yuan, X. Zhang, O. A. Scherman, *Acc. Chem. Res.* **2014**, *47*, 2106.
[27] Y.-H. Gong, C. Li, J. Yang, H.-Y. Wang, R.-X. Zhuo, X.-Z. Zhang, *Macromolecules* **2011**, *44*, 7499.

[28] P. Neirynck, J. Brinkmann, Q. An, D. W. J. van der Schaft, L.-G. Milroy, P. Jonkheijm, L. Brunsveld, *Chem. Commun.* **2013**, *49*, 3679.
[29] S. Sankaran, M. C. Kiren, P. Jonkheijm, *ACS Nano* **2015**, *9*, 3579.
[30] R. J. Pieters, *Org. Biomol. Chem.* **2009**, *7*, 2013.
[31] X.-Y. Zhu, B. Holtz, Y. Wang, L.-X. Wang, P. E. Orndorff, A. Guo, *J. Am. Chem. Soc.* **2009**, *131*, 13646.
[32] W. E. Thomas, E. Trintchina, M. Forero, V. Vogel, E. V. Sokurenko, *Cell* **2002**, *109*, 913.
[33] L. M. Nilsson, W. E. Thomas, E. V. Sokurenko, V. Vogel, *Appl. Environ. Microbiol.* **2006**, *72*, 3005.
[34] J. Lagona, P. Mukhopadhyay, S. Chakrabarti, L. Isaacs, *Angew. Chem. Int. Ed.* **2005**, *44*, 4844.
[35] F. Tian, D. Jiao, F. Biedermann, O. A. Scherman, *Nat. Commun.* **2012**, *3*, 1207.
[36] J. Brinkmann, S. Sankaran, S. Rinnen, F. H. Arlinghaus, J. De Boer, P. Jonkheijm, unpublished.
[37] B. T. Houseman, E. S. Gawalt, M. Mrksich, *Langmuir* **2003**, *19*, 1522.
[38] A. A. Brian, H. M. McConnell, *Proc. Natl. Acad. Sci. USA* **1984**, *81*, 6159.
[39] L. K. Tamm, H. M. Mcconnell, *Biophys. J.* **1985**, *47*, 105.
[40] K. Glasmastar, C. Larsson, F. Hook, B. Kasemo, *J. Colloid Interface Sci.* **2002**, *246*, 40.
[41] G. van Meer, D. R. Voelker, G. W. Feigenson, *Nat. Rev. Mol. Cell Biol.* **2008**, *9*, 112.
[42] C. J. Huang, N. J. Cho, C. J. Hsu, P. Y. Tseng, C. W. Frank, Y. C. Chang, *Biomacromolecules* **2010**, *11*, 1231.
[43] B. van Lengerich, R. J. Rawle, S. G. Boxer, *Langmuir* **2010**, *26*, 8666.
[44] C. J. Huang, P. Y. Tseng, Y. C. Chang, *Biomaterials* **2010**, *31*, 7183.
[45] S. S. Dixit, A. Szmodis, A. N. Parikh, *ChemPhysChem* **2006**, *7*, 1678.
[46] J. Page, B. A. Heitz, J. R. Joubert, J. P. Keogh, T. Sparer, S. S. Saavedra, W. He, *J. Biomed. Mater. Res. A* **2011**, *97*, 212.
[47] J. W. Lee, S. Samal, N. Selvapalam, H.-J. Kim, K. Kim, *Acc. Chem. Res.* **2003**, *36*, 621.
[48] S. Daniel, A. J. Diaz, K. M. Martinez, B. J. Bench, F. Albertorio, P. S. Cremer, *J. Am. Chem. Soc.* **2007**, *129*, 8072.
[49] H. Jung, A. D. Robison, P. S. Cremer, *J. Am. Chem. Soc.* **2009**, *131*, 1006.
[50] S. L. Harris, P. A. Spears, E. A. Havell, T. S. Hamrick, J. R. Horton, P. E. Orndorff, *J. Bacteriol.* **2001**, *183*, 4099.
[51] C. Stoffelen, J. Huskens, *Chem. Commun.* **2013**, *49*, 6740.

Q1 **APT to AU: Please provide the highest academic title (either Prof. or Dr.) for all authors, where applicable.**

Q2 **APT to AU: If you have not returned the color cost confirmation form already, please email the completed form to the editorial office when you submit your proof corrections. This will confirm that you are willing to support the cost for color publication of the figures. Details about our color policies and a link to the form were included with your acceptance email. If you wish for your figures to be presented in greyscale, please email the editorial office to confirm this.**

Q3 **APT to AU: Please provide the journal title, volume and page number for ref. (36) if now available.**